diversity

MDPI

Article

The Role of Ecological Niche Divergence in Shaping Hybridization Patterns in *Testudo graeca*

Neda Ranjbar [1], Mansoureh Malekian [1], Mohammad Reza Ashrafzadeh [2,3], Szilvia Kusza [4,*] and Mahmoud-Reza Hemami [1]

[1] Department of Natural Resources, Isfahan University of Technology, Isfahan 8415683111, Iran; n.ranjbar@alumni.iut.ac.ir (N.R.); mmalekian@iut.ac.ir (M.M.); mrhemami@iut.ac.ir (M.-R.H.)
[2] Department of Environmental Sciences, Faculty of Natural Resources and Earth Sciences, Shahrekord University, Shahrekord 8818634141, Iran; mrashrafzadeh@sku.ac.ir
[3] Research Institute of Biotechnology, Shahrekord University, Shahrekord 8818634141, Iran
[4] Centre for Agricultural Genomics and Biotechnology, Faculty of Agricultural and Food Sciences and Environmental Management, University of Debrecen, Egyetem tér 1, 4032 Debrecen, Hungary
* Correspondence: kusza@agr.unideb.hu

Abstract

Determining evolutionary significant units (ESUs) is essential for the purpose of biological conservation. Recent definitions of ESUs stress the importance of using ecological data with molecular analysis. The present work aimed to study the genetic structure and ecological niche of the spur-thighed tortoise (*Testudo graeca*) in its contact zone, with a special focus on hybridization between *T. g. buxtoni* and *T. g. zarudnyi* in Central Iran using a combination of genetic data (microsatellite markers) and ecological niche modeling (ENM). Our results indicated that despite the distinct mitochondrial clades, nuclear markers reveal gene flow between the two subspecies, especially in the contact zone, with the majority of hybrids belonging to *T. g. zarudnyi*. The genetic structure of *T. graeca* reflects a complex interplay of ancient vicariance and recent gene flow. While mitochondrial markers suggest long-term separation, nuclear markers reveal more recent hybridization events. The results obtained from ENMs demonstrated the niche differentiations. Climatic variables, such as annual rainfall and temperature seasonality, primarily drive the distribution of both subspecies. The western clade is associated with higher precipitation and lower temperature variability. These findings suggest that both subspecies hold valuable evolutionary and conservation issues. Based on these mentioned results, we strongly recommend assigning the two subspecies as ESUs to enhance the accuracy of conservation measurements. We believe that understanding the ecological factors influencing species distribution, along with molecular analysis under the recent concept of ESUs, can provide valuable insights into the conservation and management of the *T. graeca* complex in its wide geographic range.

Keywords: evolutionary significant units (ESUs); ecological niche modeling (ENM); genetic structure; hybrid zone; microsatellite loci; niche overlap; spur-thighed tortoise

Academic Editors: Jordi López-Pujol and Luc Legal

Received: 3 August 2025
Revised: 5 September 2025
Accepted: 9 September 2025
Published: 17 September 2025

Citation: Ranjbar, N.; Malekian, M.; Ashrafzadeh, M.R.; Kusza, S.; Hemami, M.-R. The Role of Ecological Niche Divergence in Shaping Hybridization Patterns in *Testudo graeca*. *Diversity* **2025**, *17*, 653. https://doi.org/10.3390/d17090653

1. Introduction

Determining evolutionary significant units (ESUs) is essential for the purpose of biological conservation. Recognizing these units allows conservation efforts to move beyond species-level protection and addressed intraspecific diversity, which is critical for maintaining evolutionary resilience in the face of environmental change [1]. However, knowing

about evolutionary forces at varied temporal scales is not enough for conservation measurements. Most species are typically divided by the environment [2]. Therefore, divergent adaptive processes between taxa is not fully clarified by DNA analysis [1]. Conservation policies can sometimes need non-molecular studies to generate critical information addressing the adaptive variations [1].

ENM is widely employed to predict species distributions [3]. While traditional ENMs assume genetic uniformity, incorporating genetic variability and local adaptation enhances model performance [4,5] and aids in identifying the processes shaping population structure and potential areas for conservation prioritization [6,7].

Geographical distance and unsuitable environmental conditions can restrict gene flow between populations, leading to distinct genetic groups. Consequently, current species distributions may reflect historical vicariance events [8]. Climate also plays a crucial role in adaptive differentiation, influencing genetic evolution by limiting dispersal and colonization in species with extensive geographic ranges. Variations in temperature, precipitation, and seasonality can create environmental gradients promoting population divergence [9,10].

The spur-thighed tortoise (*Testudo graeca*) is widely distributed across North Africa, Southern Europe and Southwest Asia, including the Caucasus and regions of Georgia, Armenia, Azerbaijan, and Iran. The taxonomic status of the *T. graeca* complex, which experiences different contact zones within its distribution range, has not been clearly established [11]. This species faces several threats, including habitat destruction, egg harvesting and the pet trade [12,13]. These factors have contributed to its Vulnerable status on the IUCN Red List and its inclusion in Appendix II of CITES.

Genetic and morphological differentiation among geographically isolated populations of *T. graeca* is well-documented. Molecular studies have identified distinct clades corresponding to recognized subspecies, with admixed populations occurring in contact zones [14–16]. While previous research has investigated gene flow between mitochondrial lineages using nuclear markers, such as AFLP and microsatellites [11,17], the easternmost regions of the species' distribution range, particularly in Iran, remain understudied.

Three subspecies are currently recognized in Iran based on mitochondrial lineages: *T. g. buxtoni*, *T. g. armeniaca*, and *T. g. zarudnyi* [15,18]. A recent phylogeographic study confirmed the presence of two divergent mitochondrial clades in Iran, corresponding to *T. g. buxtoni* and *T. g. zarudnyi* as the most ancient subspecies of the *T. graeca* complex, with a contact zone located in Central Iran. Three divergent subclades were also identified for *T. g. buxtoni* within the contact zone [19]. Although mitochondrial divergence is supported by morphological variability, the taxonomic status of the *T. graeca* complex remains unsolved. Moreover, the spatial hybridization patten within the contact zone is completely unclear. Therefore, microsatellite markers can be utilized to assess genetic structure and gene flow between the subspecies. This is critical for delineating ESUs, understanding demographic history, and guiding conservation strategies [11].

Although molecular studies have definitely done a lot to enhance our understanding of *Testudo graeca* taxonomy, the genetic structure of populations is primarily shaped by a complex interplay of biological and ecological factors, such as geographical barriers, ecological isolation and reproductive constraints [20,21]. Moreover, the species experience different contact zones in its wide range [11]. When divergent taxa come into contact, hybrid zones emerge, providing valuable natural laboratories for studying hybridization and isolation mechanisms [22]. Therefore, knowing about reproductive isolation units as we described biological species cannot fulfill our expectation. Biological species concept overlooks multiple divergence dimensions like genetic, ecological, and morphological

differentiations that can occur without complete reproductive isolation. Therefore, it hinders our understanding of biodiversity patterns particularly in contact zones.

Contact zones are often ecologically sensitive and genetically diverse. Therefore, integrating genetic data with environmental variables offers a powerful approach for exploring the spatial patterns of intraspecific genetic variation within contact zones [7]. Recent definitions of ESUs stress the importance of using ecological data with molecular analysis. This integrative approach enhances the resolution of conservation measurements, ensuring that management strategies preserve both evolutionary potential and functional diversity across heterogeneous landscapes [1,23,24].

Given the limited dispersal ability of tortoises, understanding their ecological requirements and adaptations to local environmental conditions is essential for determining the taxonomic status of the genetic clusters. The previous ecological study focused on ecological differentiation modeling between subspecies [25], whereas our research studied how ecological niche divergence shapes hybridization patterns that is a distinct evolutionary question. Our work complements the earlier study by examining the ecological mechanisms driving hybrid zone dynamics rather than simply mapping distributions. This approach is particularly important because ecological analysis of hybridization zones requires careful attention, as the patterns observed can significantly affect discussions of taxonomic status. In some cases, rather than primary contact between previously isolated forms, hybrid forms themselves may disperse, leading to wide and extended zones of intergradation.

This study aims to (1) fill the knowledge gap regarding the genetic structure and gene flow between the two mtDNA lineages by analyzing 10 polymorphic microsatellite loci; (2) identify the ecological niche overlap, divergence and factors influencing their spatial distribution in their contact zone; (3) assess the similarity and overlap of their climatic niches; and (4) compare the genetic clusters with non-molecular data to clarify whether these ancient subspecies represent distinct ESUs or have relatively identical characteristics.

2. Materials and Methods

2.1. Ethic Statement

All experiments are approved by the Iranian Department of Environment (DOE) under permission No. 97/6549. Further, all experimental protocols adhered to the ethical recommendations outlined in the ARRIVE guidelines [26].

2.2. Sampling

Samples of the two mitochondrial lineages, *T. g. buxtoni* and *T. g. zarudnyi*, were collected from the Zagros and Irano-Touranian eco-regions in Central Iran (Figure 1). Sampling was conducted over two consecutive years (2018 and 2019) during the species' active period. Individuals were tracked in their habitat using environmental guards and local people's help. Then, we captured adults of more than 12 years old. Adults were recognized by counting growth rings on the costal scales of the carapace [27].

The biopsy sampling technique, which is a non-destructive, rapid and safe method, was employed to minimize the risk of bleeding and infection [28]. However, alcohol (95%) was used before and after the sampling process. Individuals were sampled and released at the point of capture with no harm. The collected tissue was immediately preserved in pure 99% ethanol. A total of 40 adult tortoises (Table S1), comprising 15 males and 25 females, were prepared for genotyping.

2.3. Laboratory Procedures

Genomic DNA was extracted from tissue samples using the WizPrep™ gDNA MiniKit (Cell/Tissue) (WizBio Solutions Incorporated, Seongnam-si, Gyeonggi-do, Republic of

Korea). The extraction was in accordance with the manufacturer's instructions. Genotypic data were obtained for ten microsatellite loci. Ten pairs of primers were utilized, along with two sequences: CAG (CAGTCGGGCGTCATCA) and PIG (GTTT) for the forward and reverse primers, respectively (Table 1). The CAG sequence was used to label the forward primer binding site at the 5′ end with three fluorescent dyes: FAM, HEX, and TAMRA (Bio Acts Co., Ltd. Namdong-gu, Incheon, Republic of Korea) [29]. The addition of the PIG sequence at the 5′ end of the reverse primer is intended to prevent the formation of a null allele due to the addition or absence of an adenine nucleotide [30].

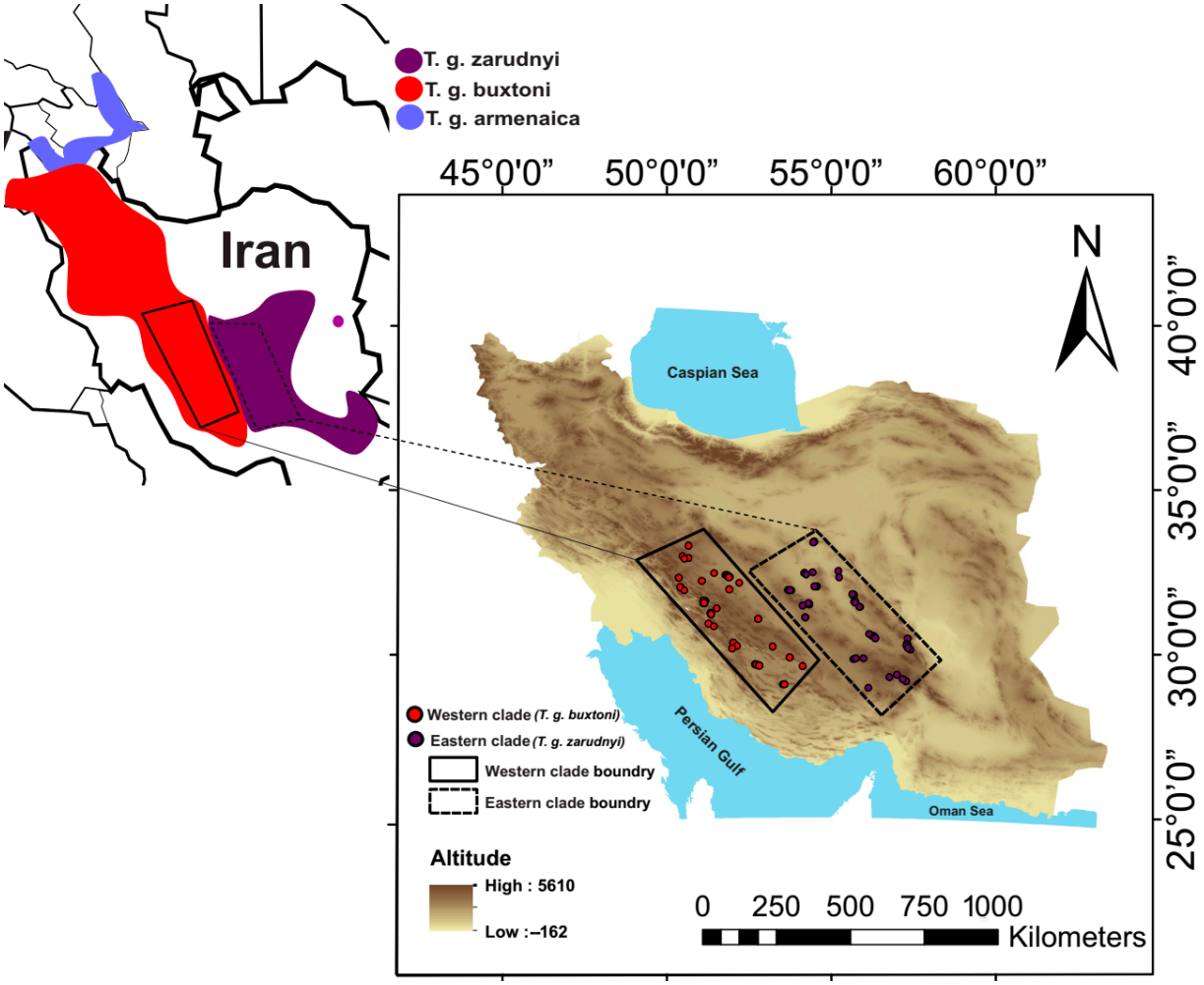

Figure 1. The distribution range of three subspecies (*T. g. buxtoni*, *T. g. zarudnyi* and *T. g. armenaica*) of *Testudo graeca* in Iran, assigned by mitochondrial clades in previous studies [19] with the connection of sampling localities of *T. g. buxtoni* (western clade) and *T. g. zarudnyi* (Eastrn clade) in Zagros and Irano-Turanian Eco-regions. The base map was sourced from ©OpenStreetMap contributors "https://www.openstreetmap.org (accessed on 10 February 2024)", available under the Open Database License (ODbL) "www.openstreetmap.org/copyright (accessed on 10 February 2024)" and created using ArcGIS version 10.5.

Ten microsatellite loci were amplified in two successive PCR reactions. The first-round PCR reaction used 7.5 µL of 2X PCR mix (Ampliqon A/S, Odense, Region of southern Denmark, Denmark), 3 mM MgCl2, 0.4 U/µL Taq DNA polymerase, 0.5 µM of each primer, and 100 ng of DNA in a total volume of 15 µL. The PCR program consisted of an initial denaturation at 95 °C for 5 min followed by 35 cycles of denaturation at 94 °C for 30 s, annealing at 64 °C for 30 s, and extension at 72 °C for 30 s, with a final extension at 72 °C for 5 min. In the second-round PCR, 0.4 µM UFL primer (TAMRA, HEX, and FAM), 0.4 µM

reverse primer, 1 µL of a 1/10 diluted PCR product from the previous step, and 7.5 µL of 2X PCR mix were added to a total volume of 15 µL. The PCR program was similar to the first round, with an initial denaturation at 95 °C for 5 min followed by 35 cycles of denaturation at 94 °C for 30 s, annealing at 60 °C for 30 s, and extension at 72 °C for 30 s, with a final extension at 72 °C for 5 min.

Table 1. The primers used in the amplification of microsatellite loci of *Testudo graeca* in Central Iran.

Code	Locus Name	Sequence	Product Size (bp)	Annealing Temperature (°C)	Reference
1	Goag6-F	TAAGGGCTATGAGGAAGAAT	369–399	53	Edwards et al. (2003) [31]
	Goag6-R	GTAATGGTGTGGGTGGGA			
2	GmuB08-F	CTCTGAGACCCTTATTCACGTC	236–262	58	King and Julian (2004) [32]
	GmuB08-R	AGCCTTTGTCTGTAAGCTGTT C			
3	Gp61-F	GCATTAAACCATTGTGCCTCA	218–236	60	Schwartz et al. (2003) [33]
	Gp61-R	AGTGGTGGTCGAAGTGGAAC			
4	Test76-F	GAATTCTAACTTTTCTCTGTGGAGC	123–145	58	Forlani et al. (2005) [34]
	Test76-R	TCTTATTGCATATCTGAGTACAGAAG			
5	Gp81-F	TCACACAAACCCCATCCATA	379–385	57	Schwartz et al. (2003) [33]
	Gp81-R	TCCATTGAATTGCCATCTGA			
6	Test56-F	GATATGCAGGCAAACAGGCT	170–234	56	Forlani et al. (2005) [34]
	Test56-R	CAGGAATCTGTGCATGATTGA			
7	Test71-F	GATTGTGGTCACATATAGAGGAGG	117–155	56	Forlani et al. (2005) [34]
	Test71-R	TGTTGTACTTAGCTGTTCTGATCTATT			
8	GmuD51-F	GTTGGGCACTAGATAGATTCG	134–220	58	King and Julian (2004) [32]
	GmuD51-R	CATTCAAGTCAACGGAAAGAC			
9	TWS190-F	TTGTTCTGCCATCAGTCAGC	94–110	62	Perez et al. (2006) [35]
	TWS190-R	ATCCCCTTACCACCAACTCC			
10	TWI61-F	TATTTCAGGCGTGGAGCAAC	247–335	62	Perez et al. (2006) [35]
	TWI61-R	CAATGGGCTACTTGCCTACC			

A 2% agarose gel was used to confirm the quality of the PCR products. For each specimen, 3–5 µL was multiplexed from each locus (depending on PCR intensity and FAM-HEX-TAMRA label). Fragment analysis was conducted on a capillary sequencer 3730XL (ABI, Thermo Fisher Scientific, Waltham, MA, USA), in the presence of GSc-Liz500 (Thermofisher Scientific, Waltham, MA, USA). Achieved chromatograms were evaluated and genotyped using the microsatellite plugin 1.4.6 of GENEIOUS IR9 software [36].

2.4. Genetic Diversity Analysis

The presence of null alleles, scoring errors, and large-allele dropout was assessed using MicroChecker version 2.2.3 [37] and FreeNA version 2009.11.16 [38]. Tests for deviations from Hardy–Weinberg equilibrium (HWE) and linkage disequilibrium between loci were conducted using the program GENEPOP version 3.4 [39]. The significance of both tests was evaluated using the Markov Chain Monte Carlo (MCMC) algorithm [40]. The resulting *p*-values were adjusted for multiple comparisons using the sequential Bonferroni correction [41]. Genetic diversity within populations was characterized by calculating the number of alleles (Na), allele size range, number of effective alleles (Ne), polymorphic information content (PIC), Shannon information index (I), observed (Ho) and expected (He) heterozygosity, unbiased expected heterozygosity (uHe), and fixation index (F_{ST}) for each locus in each population using POPGENE version 1.32 [42].

2.5. Population Structure Analysis

The Bayesian clustering method implemented in STRUCTURE version 2.1 1 [43] was used to infer the genetic structure of the tortoise populations. An admixture ancestry model with correlated allele frequencies was selected [44] due to the contact zone nature and potential connectivity among populations. No prior population information was provided. The MCMC analysis consisted of an initial burn-in period of 100,000 iterations followed by a run of 100,000 iterations. Ten independent runs for each K (the number of genetic clusters) ranging from 1 to 5 were conducted. The mean estimated posterior probability, Ln P(X/K), was calculated for each K. The optimal value of K was determined using both the original method by Prichard et al. [38] and the method proposed by Evanno et al. [45], where the highest ΔK score represents the optimal number of clusters. This analysis was performed using Structure Harvester version 0.6.93 [46]. CLUMPP 1.1.2 [47] was used to calculate the average membership probability for each sample across the 10 independent runs for each K, while DISTRUCT version 1.1 [48] was employed to visualize the genetic clusters.

2.6. Population Differentiation and Gene Flow

The F_{ST} index was calculated for each locus individually, as well as for the two mtDNA clades, using the method developed by Weir and Cockerham [49]. To address potential bias, F_{ST} values were corrected for null alleles using the weighted variance analysis method of Weir and Cockerham in FreeNA version 2009.11.16 software. This correction included a 95% confidence interval and involved 10,000 repetitions of the calculation. Subsequently, gene flow (Nm) between populations was estimated based on the corrected F_{ST} index.

The inbreeding coefficient (FIS) was determined for each locus within each population, as well as for all loci combined, using a general estimate of this index through the Weir and Cockerham method in GENEPOP version 3.4 software.

2.7. Identification of Dispersal Events

GeneClass version 2 [50] with the Bayesian method of Rannala & Mountain [51] was employed to identify first-generation migrants. A Monte Carlo re-sampling approach with 10,000 simulations and a significance level of 0.05 was used. We utilized L = L_home and L = L_home/L_max models to estimate migrant probability

2.8. Ecological Niche Modeling

A total of 111 occurrence points were utilized for ENM, comprising 54 localities for *T. g. zarudnyi* and 57 localities for *T. g. buxtoni* (Figure 1). The recorded points were spaced at least 2 km apart to minimize the effects of spatial autocorrelation.

Environmental variables were selected based on a literature review of the genus Testudo [52–55] and field surveys of habitat characteristics in Central Iran. We included 19 bioclimatic variables from the WorldClim dataset [56], five topographic variables (elevation, aspect, slope, ruggedness, and solar radiation) derived from a digital elevation model (DEM), two vegetation-related variables (land cover and NDVI), and five soil physical structure variables (bulk density, clay content, coarse fragments, sand, and silt). Topographic variables were generated using ArcGIS version 10.5, and land cover data was extracted from a land use/land cover map created by the Iranian Forests, Rangelands, and Watershed Management Organization (IFRWO). Soil data was downloaded from Soil Grids.org.

We identified significant variables by conducting a preliminary Maximum Entropy model that included all variables, allowing us to determine those with high permutation importance and a logical relationship with habitat suitability. Pearson's correlation tests were performed among the layers to assess multicollinearity, using a threshold value of 0.75. Layers exhibiting high correlation that were not recognized as important variables

were subsequently removed. The final ENM runs included 10 variables: temperature annual range, precipitation seasonality, DEM, slope, solar radiation, NDVI, distance from shrublands, soil bulk density, soil clay content and soil coarse fragments.

To generate habitat suitability maps for each subspecies, we conducted ensembles of small models (ESMs) [57,58] using the R package sdm version 1.0-81 [59]. Six species distribution models (SDMs) were combined in the ESMs: random forest (RF), generalized linear model (GLM), Maximum Entropy (MaxEnt), generalized boosting model (GBM), generalized additive model (GAM), and multivariate adaptive regression spline (MARS).

For each subspecies, a 10-fold cross-validation approach was used to replicate the modeling based on randomly selected background and occurrence points. Two sets of 5000 background points were randomly selected for each subspecies. We used 75% of occurrences as training data and 25% as evaluation data. The predictive performance of the models was evaluated using Cohen's kappa coefficient, true skill statistics (TSS), and the area under the curve (AUC) of a receiver operating characteristic (ROC). The final ESM was evaluated by weighted-averaging the individual SDMs proportionally to their predictive accuracy. To produce classified suitability maps, the minimum suitability value at occurrence localities was used as a threshold. The role of each variable in predicting the distribution of each subspecies was also determined by averaging the related scores across all SDMs.

2.9. Niche Divergence

To estimate the climatic niche similarity between the subspecies, we utilized the Environmental principal component analysis (PCA-env) approach [60] using PCs extracted from 19 climatic variables in Ecospot package in R version 4.1.3. Both occurrences and background niche must be used to calculate multivariate climate axes. For the background niche, a 20 km circular buffer around the occurrences was defined to ensure that all accessible areas within the contact zone were covered for each subspecies. On the other hand, the buffer cannot be expanded to exclude the other contact zones that may occur with *T. g. armeniaca* in the west and *T. hermanni* in the east part of the study area. This buffer was then used as a mask layer to prepare 19 bioclimatic variables for PCA analysis. In the first step of this analysis, the Kernel density function was used to calculate the density of occurrences and climate variables in the multivariate PCA space. In the second step, niche overlap was computed across the gradient of the PCA for two subspecies using Schoener's D metric. Finally, two randomization procedures of niche equivalency and niche similarity were used to check the hypotheses of niche divergence/conservatism [60].

3. Results

3.1. Genetic Diversity

No significant large-allele dropout errors or null alleles were detected using MicroChecker and FreeNA. Four loci (Test71, Test76, Test81, and GmuB08) showed some departure from HWE (p = 0.01), but these results were not significant after Bonferroni correction for each population (α = 0.005). No significant linkage disequilibrium was observed between 90 pairwise comparisons of loci considering each population separately and 45 pairwise comparisons for both populations.

Genetic diversity metrics are presented in Table 2. The number of alleles varied from 3 to 12, and the number of effective alleles ranged from 1.17 to 7.26. There were no significant differences in allelic richness and unbiased heterozygosity [61] between the two clades (F = 1.2, p = 0.43, and F = 0.35, p = 0.8, respectively). Overall, the inbreeding rate for both populations was low, with the eastern clade, primarily related to *T. g. zarudnyi*, showing lower inbreeding coefficients.

Table 2. Summary statistics of genetic diversity for ten loci in each population of *Testudo greaeca* in Central Iran.

Locus	Population	Na	Allele Size Range	Ne	PIC	I	Ho	He	uHe	F_{IS}	F_{ST}	Corrected F_{ST}
Test76	G1	3	131–145	1.22	0.17	0.37	0.04	0.177	0.18	0.79	0.78	−0.02
	G2	3	112–139	1.24	0.19	0.41	0.04	0.196	0.20	0.66	0.64	
Gp61	G1	3	218–236	2.16	0.43	0.83	0.96	0.536	0.55	−0.79	−0.79	0.00
	G2	3	218–236	2.12	0.42	0.82	0.93	0.528	0.55	−0.74	−0.76	
GmuB08	G1	6	234–262	4.04	0.71	1.54	0.46	0.752	0.77	0.32	0.39	0.02
	G2	10	234–262	7.26	0.85	2.12	0.71	0.862	0.89	0.13	0.17	
Goag6	G1	7	361–399	2.21	0.50	1.15	0.50	0.547	0.56	0.00	0.09	0.02
	G2	8	373–397	3.77	0.71	1.68	0.71	0.735	0.76	−0.06	0.03	
Test71	G1	6	117–155	1.58	0.35	0.84	0.35	0.37	0.37	−0.11	0.06	0.38
	G2	8	119–151	3.70	0.70	1.66	0.36	0.73	0.75	0.54	0.51	
Test56	G1	7	174–234	2.97	0.66	1.33	0.88	0.66	0.67	−0.55	−0.33	0.09
	G2	12	170–232	6.88	0.85	2.19	0.71	0.85	0.88	0.00	0.16	
Gp81	G1	3	379–385	1.17	0.14	0.31	0.07	0.14	0.15	0.74	0.73	0.00
	G2	3	379–385	1.57	0.31	0.62	0.28	0.35	0.36	0.22	0.18	
TWS190	G1	3	94–110	2.06	0.40	0.77	0.77	0.51	0.52	−0.48	−0.49	0.01
	G2	4	94–110	2.20	0.48	0.94	0.64	0.54	0.56	−0.15	−0.18	
GmuD51	G1	11	136–220	3.93	0.77	1.77	0.65	0.75	0.76	0.14	0.12	0.01
	G2	10	134–202	2.58	0.61	1.51	0.50	0.61	0.64	0.22	0.18	
TWI61	G1	3	303–335	2.16	0.43	0.83	0.96	0.54	0.55	−0.79	−0.79	0.00
	G2	5	247–335	2.65	0.55	1.15	0.96	0.62	0.65	−0.58	−0.61	

Values include the number of alleles (Na), allele size range, number of effective alleles (Ne), polymorphic information content (PIC), Shannon information index (I), observed heterozygosity (Ho), expected heterozygosity (He), unbiased expected heterozygosity (uHe), Inbreeding coefficient (F_{IS}), and fixation index (F_{ST}) for two populations (G1 and G2).

3.2. Population Structure

Mean LnP(D) and ΔK were calculated for K values ranging from 1 to 5 across 10 independent runs. Both Mean LnP(D) and ΔK increased up to K = 2 and subsequently decreased (Table 3). The consistency of the estimated probability of the data (Ln P(X/K)) across different runs further confirmed that the chains had converged. The maximum log-likelihood value of the data was achieved at K = 2 (Ln P(X/K) = −990) and declined thereafter from K = 1 to K = 5 (Table 3). A distinct peak in ΔK was also observed at K = 2 (ΔK = 14.7), after which ΔK decreased.

Table 3. Mean log probability of data (LnP(K)) and Delta K (ΔK) for different values of K, obtained from 10 independent replications. The most likely K with the highest ΔK is in bold.

No. Population (K)	Mean LnP(K)	Stdev LnP(K)	Ln′(K)	|Ln″(K)|	ΔK
1	−956.5	0.55	-	-	-
2	**−990.2**	**10.4**	**−33/72**	**149.8**	**14.7**
3	−1173.7	43.7	−183.5	40.5	0.92
4	−1316.6	154.7	−142.9	259.8	1.6
5	−1199.7	107.2	116.7	-	-

Based on STRUCTURE analysis (Figure 2), the optimal number of populations was determined to be two. All pure samples from the western part of the contact zone were grouped into one population and related to the subspecies *T. g. buxtoni*. Pure genotypes from the eastern part, along with two samples from the central part, were grouped into another population. With the exception of one sample belonging to *T. g. buxtoni*, all of these eastern genotypes belonged to the subspecies *T. g. zarudnyi*. The accumulation of hybrid individuals was observed in the central part of the contact zone (Figure 2).

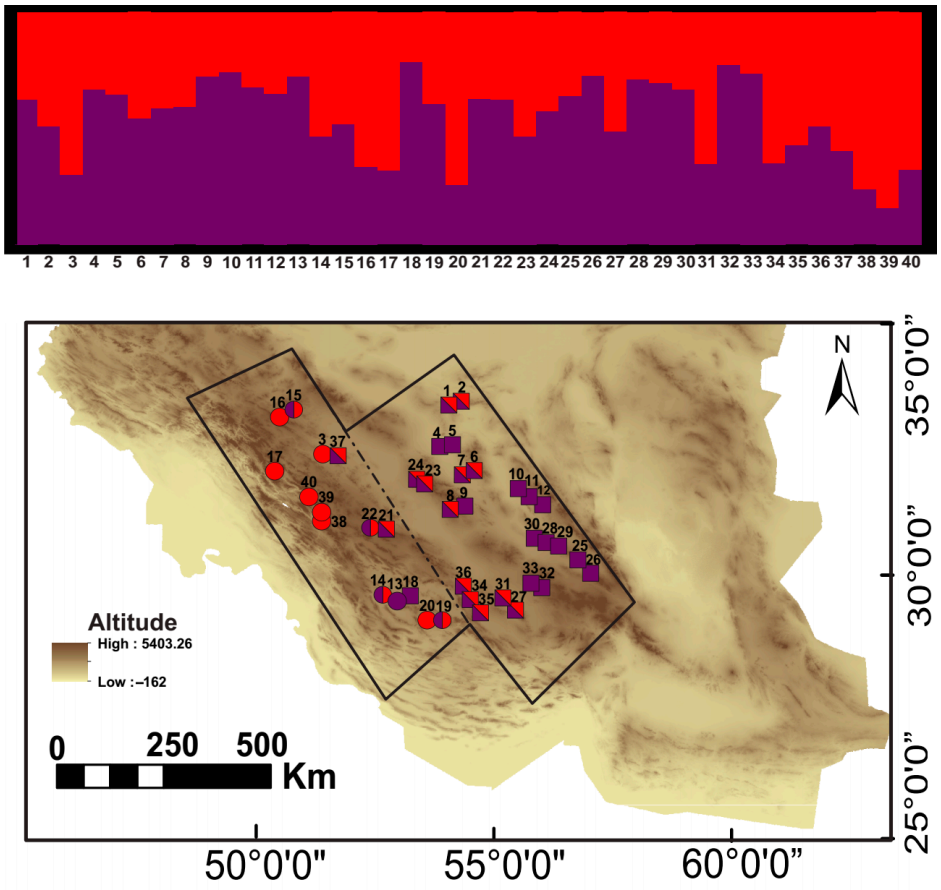

Figure 2. The bar graph represents the genotype of each individual and their location on the map. Squares and circles denote the eastern and western clades corresponding to the subspecies of *T. g. zarudnyi* and *T. g. buxtoni*. Hybrid samples are indicated based on a threshold of 65%. The base map was sourced from ©OpenStreetMap contributors (https://www.openstreetmap.org), available under ODbL (www.openstreetmap.org/copyright) and created using ArcGIS 10.5.

The gene flow index (number of migrants) was estimated based on the corrected F_{ST} between both populations, which ranged from 1.28 to 32.11.

3.3. Identification of Dispersal Events

Ten first-generation migrant dispersal events were detected across the study region ($p < 0.05$), with the geographic origin identified with high confidence (Table 4). Out of the ten putative dispersal events, five originated from the Irano-Turanian Eco-region, while the remaining five originated from the Zagros Eco-region. In contrast to the clustering results of STRUCTURE, four of the detected migrants were not hybrids. Two of these four were recognized with the L_home/L_max model, one with the L_home model, and one with both models (Table 4).

3.4. Habitat Suitability and Niche Modeling

All models performed reasonably well in predicting suitable habitats for both clades of *T. graeca* (Table 5). On average, GAM, GBM, and RF distribution models demonstrated excellent predictive performance (AUC > 0.9), while GLM, MaxEnt and MARS exhibited good performance (AUC > 0.7) according to the AUC metric. The TSS prediction accuracy was also good for all models (Table 5). Among the selected algorithms, RF exhibited the highest values (AUC = 0.99, TSS = 0.99), while GLM had the lowest (AUC = 0.68, TSS = 0.67, Table 5).

Table 4. Results of migrant detection analyses using GeneClass.

Sample	Geographic Origin	Structure Cluster (G1/G2). No Prior Population Information, K = 2	Geneclass Migrant Probability Using L_Home/L_Max (*) L_Home (**), and Both Methods (***)
6	Irano-Turanian Eco-region	0.5424, 0.4576	0.0017 ***
28	Irano-Turanian Eco-region	0.7119, 0.2881	0.0083 *
31	Irano-Turanian Eco-region	0.3475, 0.6525	0.0040 ***
36	Irano-Turanian Eco-region	0.5103, 0.4897	0.0476 *
13	Zagros Eco-region	0.7247, 0.2753	0.0462 *
14	Zagros Eco-region	0.4654, 0.5346	0.0136 *
19	Zagros Eco-region	0.6045, 0.3955	0.0061 *
22	Zagros Eco-region	0.6255, 0.3745	0.0218 *
27	Irano-Turanian Eco-region	0.4862, 0.5138	0.0143 **
39	Zagros Eco-region	0.1567, 0.8433	0.0000 **

Table 5. The mean of TSS and AUC for selected algorithms for habitat suitability modeling of the subspecies of *T. g. zarudnyi* and *T. g. buxtoni*.

	T. g. Buxtoni		*T. g. Zarudnyi*	
Model	**TSS**	**AUC**	**TSS**	**AUC**
GLM	0.70	0.68	0.67	0.70
MaxEnt	0.71	0.85	0.81	0.92
GBM	0.91	0.98	0.89	0.97
GAM	0.90	0.95	0.93	0.96
RF	0.99	0.99	0.99	0.99
MARS	0.70	0.76	0.77	0.95

AUC: the area under the curve of a receiver operating characteristic (ROC), TSS: true skill statistic, GLM: generalized linear model, GAM: generalized additive model, GBM: generalized boosting model, RF: random forest, MARS: multivariate adaptive regression splines, RF: random forest, and MaxEnt: maximum entropy.

The most important variables for predicting habitat suitability of the western clade included clay content, soil coarse fragments, and altitude. For the eastern clade, the variables with the highest contributions to the model were clay content, slope, and bio15 (precipitation seasonality) (Table 6). Among the climatic variables, temperature annual range and precipitation seasonality were the primary factors influencing the distribution of the tortoise species. The ecological niche of both clades is characterized by higher precipitation and lower seasonal temperature variability.

The ESMs consistently predicted habitat suitability for both clades when compared with occurrence records. The classified map of habitat suitability for the two clades (Figure 3) revealed that the eastern clade had a wider distribution with greater suitable habitats across the study area, while the suitable habitats for the western clade were mostly concentrated in the Zagros eco-region with a 0.91% habitat overlap. This overlap primarily occurred near the center of the contact zone, where the presence of hybrid individuals was confirmed. However, limited overlap was observed in the eastern part of the contact zone (Figure 3). Overall, the relative habitat suitability values predicted by the ESM for both clades indicated their niche separation.

3.5. Niche Divergence

The PCA-env revealed that the first two axes accounted for 77.7% of the total variation in climatic conditions across the two clades (PC1 = 54.2% and PC2 = 23.5%; Figure 4). The density of occurrence indicated a clear distinction between the eastern and western clades along PC1 (Figure 4A,B). Furthermore, the eastern clade was found to occupy a broader range compared to the western clade. The comparison of the relative contributions of variables (Figure 4D), based on the PCA, demonstrated differences in the climatic characteristics of the habitats of the two clades. For instance, the niche of the western clade was characterized by higher precipitation and lower temperature variability.

Table 6. Variable importance in the habitat suitability of the western and eastern clades of *Testudo graeca*.

Variable	Variable Importance	
	Western Clade	**Eastern Clade**
Clay content	30.1	38.2
Soil coarse fragments	20.6	5.2
Altitude	18.9	6.1
Slope	2.8	19.3
bio15	6.1	16.8
bio7	2.7	2
NDVI	9.3	4
Distance from shrublands	4.5	3.8
Solar radiation	3.5	1.8
Bulk density	1.4	2.9

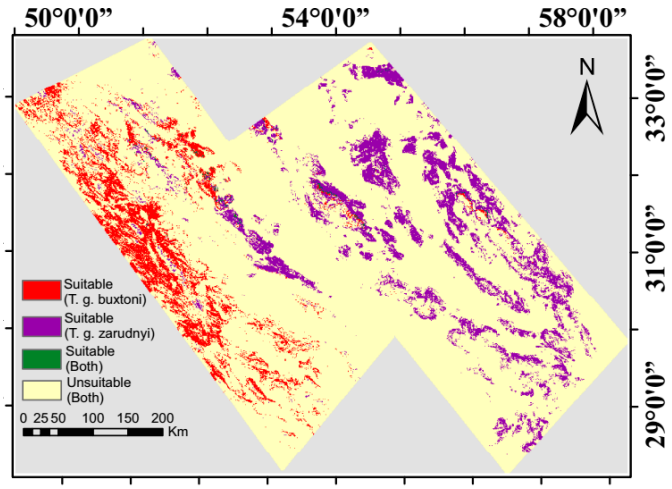

Figure 3. Classified ensemble map of habitat suitability of the two subspecies of *T. g. zarudnyi* and *T. g. buxtoni*.

A significant difference was observed between the occupied niches of the two mtDNA clades (Figure 5). The climatic niches occupied by the two clades were not statistically equivalent ($p < 0.05$), and their similarity was significantly greater than expected by chance ($p = 0.02$). Both equivalency and similarity tests demonstrated that, despite the similarities in the environmental space occupied by the lineages, the climatic niches they utilize are not the same.

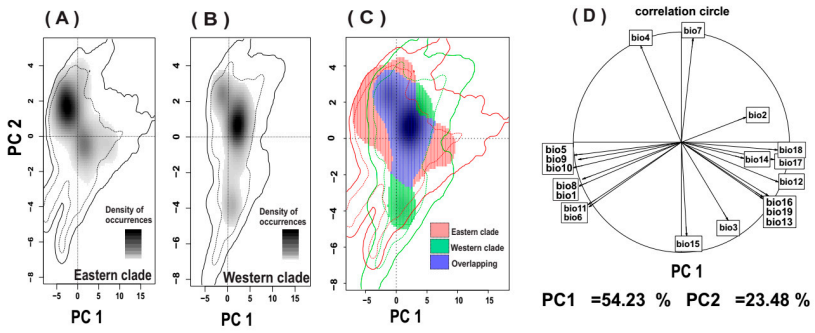

Figure 4. Climatic niches of the eastern and western clades of the tortoise in Central Iran. The dark part shows the density of occurrence of western clade (**A**) and eastern clade (**B**). The background environment of 50% and 100% better quality is shown with black and gray lines. The climatic niche overlap of the two clades (**C**). The dark blue area indicates niche overlap in both clades. (**D**): the relative contribution of climate variables along the two PC axes (PC1 and PC2).

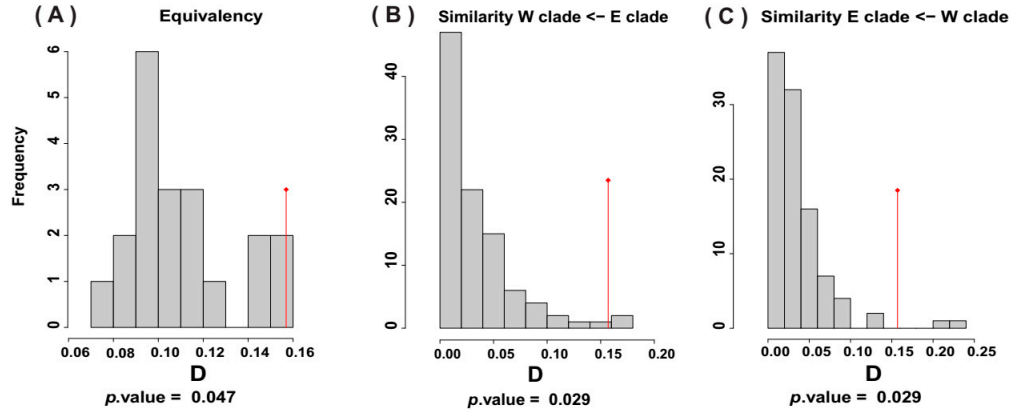

Figure 5. Equivalency (**A**) and similarity tests (**B**) and (**C**) between western (W) and eastern (E) clades. Vertical red lines and gray bars indicate observed and estimated overlap (Shaner's overlap index, D) between clades.

4. Discussion

According to our best knowledge, a combination of genetic data and ecological niche models was employed for the first time in this study to evaluate the genetic structure and gene flow between the two divergent mitochondrial clades of *Testudo graeca* distributed in Central Iran. Genetic analysis results confirmed the outcome of previous studies [16,19,62] about the separation of the two clades at the easternmost and westernmost sides of the Zagros mountain range. However, as we approached the contact zone, the proportion of migrants and hybrid individuals increased, suggesting that despite the species' limited mobility, gene flow between the lineages has been established for a significant period. In addition to ongoing admixture, active dispersal through permeable contact zone was confirmed by gene class results as four of the detected migrants were not hybrids.

The contrasting results of mtDNA sequences and microsatellite markers indicate distinct phases in the evolutionary history of *Testudo graeca*. Divergent mtDNA lineages suggest ancient vicariance events, while the microsatellites data reflect more recent episodes of gene flow [11]. Additionally, Mikulíček et al. (2013) [17] proposed that gene flow between the distinct mtDNA lineages is primarily mediated by males. The larger home ranges of male tortoises, along with their greater dispersal abilities over longer distances compared to females, can explain this mismatched pattern [63,64]. Moreover, the structure analysis revealed only one microsatellite cluster for the western clade, which conflicts with the deeply divergent mtDNA subclades identified in a previous study [19]. Therefore, relying solely on the genetic isolation of mtDNA sequences without considering nuclear markers can lead to confusing taxonomic inferences.

A significant proportion of hybrid individuals in the plains of Central Iran (Irano-Turanian Eco-region) can be attributed to the lack of biogeographical barriers, such as high mountains and rivers. An assessment of hybrid individuals in the contact zone revealed that the majority belong to the subspecies *T. g. zarudnyi*, indicating a lower inbreeding coefficient compared to others. This suggests a higher level of adaptability of this subspecies to environmental conditions. Pure individuals of the subspecies *T. g. zarudnyi* are primarily located in Kerman Province and the southern regions of Yazd Province. In contrast, pure individuals of the subspecies *T. g. buxtoni* are dispersed throughout the western and southern areas of Chaharmahal and Bakhtiari Province, maintaining a considerable distance from the center of the contact zone. This distribution pattern indicates an Isolation by Distance (IBD) scenario, where distance plays a significant role in population separation [65].

The climatic niche of the two mtDNA clades was investigated using the PCA-env approach. PCA-env reduces bios into interpretable gradients through environmental space rather than multiple variables in geographical space. This makes niche comparison more ecologically meaningful than common ENM outputs. Our results indicated that the ecological niche of the western clade is characterized by higher precipitation and lower seasonal temperature variability compared to the eastern clade. In contrast, previous niche modeling studies have used bios as multiple climatic variables in common ENM models [18,25].

Similarity and equivalency tests indicated that, despite the overlap in the environmental space occupied by the two clades, their climatic niches are not identical. The results obtained from SDMs were relatively consistent with climate niche and genetic analyses, leading to the recognition of two distinct evolutionary units. In agreement with our study, significant differentiations were observed between the two subspecies in Iran using climatic and elevation data [25]. However, we focus on the contact zone to reveal whether hybrids derived from genetic analysis occupied overlapped or novel niches, informing conservational measurements. We noted some limited overlap in the easternmost part of the contact zone, where pure individuals of the subspecies *T. g. zarudnyi* were present. This highlights the importance of studying the release of captured individuals into their natural habitats, a practice that is quite common for tortoises [13]. Without considering these differentiations, there is the possibility for increased hybridization and the loss of evolutionary divergence, particularly for the case of *T. g. zarudnyi*, which is an Iranian endemic subspecies.

Furthermore, the SDMs demonstrated less overlap and more differences compared to previous studies. This can be due to entering soil layers in addition to climatic and elevation data [18,25]. Soil type played a key role in limiting tortoise distribution that are highly dependent on ground conditions for survival, movement and reproduction [66]. Morphological divergence between the two clades was affected by soil condition and had higher impact on the eastern clade.

In open areas with limited shelter, like in the Irano-Turanian eco-region, soil, particularly clay rich soil helps tortoises to dig and penetrate the ground for egg covering and shelter [67]. Consequently, areas with lower slopes may be more suitable for the eastern clade [55], aligning with our findings regarding the significant variables identified for both clades. Moreover, environmental factors can significantly influence the lateral dimensions of the carapace and width of plastron lobes [19,67]. Mobility is essential for navigating between shelters and locating food in such environments [68]. As a result, the morphological populations associated with the plains of Iran exhibit a more flatted carapace, which is suitable for burrowing, and narrower plastron lobes providing increased space for the head, limbs, and feet, thereby enhancing mobility [69]. In contrast, the conditions for populations inhabiting the mountainous regions of the Zagros are entirely different. More suitable environmental conditions create a relatively suitable habitat for plant growth. Additionally, the mountainous landscape of these regions, with its higher altitude, offers extra shelter. Therefore, the morphological populations in this region exhibited domed carapaces, longer coastal scales, wider vertebral scales, and wider plastral lobes, indicating the availability of more suitable conditions for growth and additional shelter [19].

5. Conclusions

Overall, this study highlights the significance of contact zones as valuable opportunities for examining evolutionary processes. The separation of the two clades on the easternmost and westernmost sides of the contact zone is supported by nuclear microsatellite markers, ecological data, phylogenetic analysis, divergence times, and morphological characteristics. However, both morphological and phylogenetic evidence indicated greater

divergence between *T. g. buxtoni* and *T. g. zarudnyi* [19]. Furthermore, ecological niche models indicate an overlap that corresponds with the locations of hybrid individuals and migrants in the center of the contact zone. The observed inconsistencies among morphology, mtDNA and nDNA underscore the importance of considering different marker systems in taxonomic studies. Furthermore, the distinct habitat requirements of the subspecies, as derived from ecological modeling, remind us of the importance of using ecological data with molecular analysis in recent definitions of ESUs [1,23,24]. Conservation measurements cannot be effective when we only consider the biological species concept using molecular analysis [70]. Based on these mentioned results, we strongly recommend assigning the two subspecies as ESUs to enhance the accuracy of conservation and management.

Supplementary Materials: The following supporting information can be downloaded at: https://www.mdpi.com/article/10.3390/d17090653/s1. Table S1: Supplementary information for samples of *T. g. buxtoni* and *T. g. zarudnyi* collected in this study.

Author Contributions: N.R., M.M. and M.-R.H. conceived the ideas, N.R. collected the data, N.R. and M.R.A. analyzed the data; N.R., M.M. and S.K. led the writing with input from all other authors. All authors have read and agreed to the published version of the manuscript.

Funding: This research was funded by Iran National Science Foundation (INSF), grant number 98002534.

Institutional Review Board Statement: The study was conducted in accordance with the Declaration of Helsinki and approved by the Institutional Review Board of the Iranian Department of Environment (DOE) (protocol code 97/6549 and date of approval 12 May 2018). Further, all experimental protocols adhered to the ethical recommendations outlined in the ARRIVE guidelines [25].

Data Availability Statement: The original contributions presented in this study are included in the article/Supplementary Materials. Further inquiries can be directed to the corresponding author.

Acknowledgments: The author would like to thank the Iranian Department of Environment for sampling authorizations, park guards and local people for their assistance in sampling tortoises across the region. Supported by the University of Debrecen Program for Scientific Publication.

Conflicts of Interest: The authors declare no conflicts of interest.

Abbreviations

The following abbreviations are used in this manuscript:

ESU	Evolutionary Significant Units
ENM	Ecological Niche Modeling
DOE	Department of Environment
ODbL	Open Database License
DEM	Digital Elevation Model
IFRWO	Iranian Forests, Rangelands, and Watershed Management Organization
ESM	Ensembles of Small Models
SDM	Species Distribution Model
RF	Random Forest
GLM	Generalized Linear Model
MaxEnt	Maximum Entropy
GBM	Generalized Boosting Model
MARS	Multivariate Adaptive Regression Splines
TSS	True Skill Statistics
AUC	Area Under Curve
ROC	Receiver Operating Characteristic

HWE	Hardy–Weinberg Equilibrium
MCMC	Markov Chain Monte Carlo
Na	Number of alleles
Ne	Number of effective alleles
PIC	Polymorphic Information Content
Ho	Heterozygosity (observed)
He	Heterozygosity (expected)
uHe	unbiased Heterozygosity (expected)
IBD	Isolation by Distance
INSF	Iran National Science Foundation
PCA-env	Environmental principal component analysis

References

1. Casacci, L.P.; Barbero, F.; Balletto, E. The "Evolutionarily Significant Unit" concept and its applicability in biological conservation. *Ital. J. Zool.* **2013**, *81*, 182–193. [CrossRef]
2. Hoelzel, A.R. Where to now with the evolutionarily significant unit? *Trends Ecol. Evol.* **2023**, *38*, 1134–1142. [CrossRef]
3. Warren, D.L.; Glor, R.E.; Turelli, M. ENMTools: A toolbox for comparative studies of environmental niche models. *Ecography* **2010**, *33*, 607–611. [CrossRef]
4. Ikeda, D.; Max, T.L.; Allan, G.J.; Lau, M.K.; Shuster, S.M.; Whitham, T.G. Genetically informed ecological niche models improve climate change predictions. *Glob. Change Biol.* **2017**, *23*, 164–176. [CrossRef] [PubMed]
5. Goudarzi, F.; Hemami, M.R.; Malekian, M.; Fakheran, S.; Martínez-Freiría, F. Species versus within-species niches: A multi-modelling approach to assess range size of a spring-dwelling amphibian. *Sci. Rep.* **2021**, *11*, 597. [CrossRef]
6. Razgour, O.; Forester, B.; Taggart, J.B.; Bekaert, M.; Juste, J.; Ibanez, C.; Puechmaille, S.J.; Novella-Fernandez, R.; Alberdi, A.; Manel, S. Considering adaptive genetic variation in climate change vulnerability assessment reduces species range loss projections. *Proc. Natl. Acad. Sci. USA* **2019**, *116*, 10418–10423. [CrossRef]
7. Menon, M.; Landguth, E.; Leal-Saenz, A.; Bagley, J.C.; Schoettle, A.W.; Wehenkel, C.; Flores-Renteria, L.; Cushman, S.A.; Waring, K.M.; Eckert, A.J. Tracing the footprints of a moving hybrid zone under a demographic history of speciation with gene flow. *Evol. Appl.* **2020**, *13*, 195–209. [CrossRef]
8. Sanmartín, I. Historical biogeography: Evolution in time and space. *Evo. Edu. Outreach* **2012**, *5*, 555–568. [CrossRef]
9. Oboudi, R.; Malekian, M.; Khosravi, R.; Fadakar, D.; Adibi, M.A. Genetic structure and ecological niche segregation of Indian gray mongoose (*Urva edwardsii*) in Iran. *Ecol. Evol.* **2021**, *11*, 14813–14827. [CrossRef]
10. Li, E.; Wang, Y.; Liu, K.; Liu, Y.; Xu, C.; Dong, W.; Zhang, Z. Historical climate change and vicariance events contributed to the intercontinental disjunct distribution pattern of ash species (*Fraxinus*, *Oleaceae*). *Commun. Biol.* **2024**, *7*, 603. [CrossRef] [PubMed]
11. Mashkaryan, V.; Vamberger, M.; Arakelyan, M.; Hezaveh, N.; Carretero, M.A.; Corti, C.; Harris, D.J.; Fritz, U. Gene flow among deeply divergent mtDNA lineages of *Testudo graeca* (Linnaeus, 1758) in Transcaucasia. *Amphib.-Reptil.* **2013**, *34*, 337–351. [CrossRef]
12. Böhm, M.; Collen, B.; Baillie, J.E.; Bowles, P.; Chanson, J.; Cox, N.; Hammerson, G.; Hoffmann, M.; Livingstone, S.R.; Ram, M.; et al. The conservation status of the world's reptiles. *Biol. Conserv.* **2013**, *157*, 372–385. [CrossRef]
13. Stanford, C.B.; Iverson, J.B.; Rhodin, A.G.; van Dijk, P.P.; Mittermeier, R.A.; Kuchling, G.; Berry, K.H.; Bertolero, A.; Bjorndal, K.A.; Blanck, T.E.; et al. Turtles and Tortoises Are in Trouble. *Curr. Biol.* **2020**, *30*, R721–R735. [CrossRef]
14. Van der Kuyl, A.C.; Ballasina, D.L.; Zorgdrager, F. Mitochondrial haplotype diversity in the tortoise species *Testudo graeca* from North Africa and the Middle East. *BMC Evol. Biol.* **2005**, *5*, 29. [CrossRef]
15. Fritz, U.; Hundsdörfer, A.; Široký, P.; Auer, M.; Kami, H.; Lehmann, J.; Mazanaeva, L.; Türkozan, O.; Wink, M. Phenotypic plasticity leads to incongruence between morphology-based taxonomy and genetic differentiation in western Palaearctic tortoises (*Testudo graeca* complex; *Testudines*, *Testudinidae*). *Amphib.-Reptil.* **2007**, *28*, 97–121. [CrossRef]
16. Fritz, U.; Harris, D.J.; Fahd, S.; Rouag, R.; Martínez, E.G.; Casalduero, A.G.; Široký, P.; Kalboussi, M.; Jdeidi, T.B.; Hundsdörfer, A.K. Mitochondrial phylogeography of *Testudo graeca* in the Western Mediterranean: Old complex divergence in North Africa and recent arrival in Europe. *Amphib.-Reptil.* **2009**, *30*, 63–80. [CrossRef]
17. Mikulíček, P.; Jandzik, D.; Fritz, U.; Schneider, C.; Široký, P. AFLP analysis shows high incongruence between genetic differentiation and morphology-based taxonomy in a widely distributed tortoise. *Biol. J. Linn. Soc.* **2013**, *108*, 151–160. [CrossRef]
18. Javanbakht, H.; Ihlow, F.; Jablonski, D.; Široký, P.; Fritz, U.; Rödder, D.; Sharifi, M.; Mikulíček, P. Genetic diversity and Quaternary range dynamics in Iranian and Transcaucasian tortoises. *Biol. J. Linn. Soc.* **2017**, *121*, 627–640. [CrossRef]
19. Ranjbar, N.; Malekian, M.; Ashrafzadeh, M.R.; Hemami, M.R. Phylogeographic and phenotypic divergence between two subspecies of *Testudo graeca* (*T. g. buxtoni* and *T. g. zarudnyi*) across their contact zone in Iran. *Sci. Rep.* **2022**, *12*, 13579. [CrossRef]

20. Bradburd, G.S.; Coop, G.M.; Ralph, P.L. Inferring continuous and discrete population penetic structure across space. *Genetics* **2018**, *210*, 33–52. [CrossRef]
21. Blankers, T.; Shaw, K.L. The biogeographic and evolutionary processes shaping population divergence in Laupala. *Mol. Ecol.* **2024**, *33*, e17444. [CrossRef] [PubMed]
22. Johannesson, K.; Le Moan, A.; Perini, S.; André, C.A. darwinian laboratory of multiple contact zones. *Trends Ecol. Evol.* **2020**, *35*, 1021–1036. [CrossRef]
23. Crandall, K.A.; Bininda-Emonds, O.R.; Mace, G.M.; Wayne, R.K. Considering evolutionary processes in conservation biology. *Trends Ecol. Evol.* **2000**, *15*, 290–295. [CrossRef]
24. de Guia, A.P.O.; Saitoh, T. The gap between the concept and definitions in the Evolutionarily Significant Unit: The need to integrate neutral genetic variation and adaptive variation. *Ecol. Res.* **2007**, *22*, 604–612. [CrossRef]
25. Hosseinian Yousefkhani, S.S.; Faizi, H.; Taghipour, A.A. Modeling ecological differentiation in the distribution patterns of two subspecies of the Greek Tortoise, *Testudo graeca* (*Reptilia*: *Testudinidae*) in Iran. *Zool. Middle East* **2024**, *71*, 22–31. [CrossRef]
26. Percie du Sert, N.; Ahluwalia, A.; Alam, S.; Avey, M.T.; Baker, M.; Browne, W.J.; Clark, A.; Cuthill, I.C.; Dirnagl, U.; Emerson, M.; et al. Reporting animal research: Explanation and elaboration for the ARRIVE guidelines 2.0. *PLoS Biol.* **2020**, *18*, e3000411. [CrossRef]
27. Filippi, E.; Rugiero, L.; Capula, M.; Burke, R.L.; Luiselli, L. Population and thermal ecology of *Testudo hermanni hermanni* in the Tolfa Mountains of Central Italy. *Chelonian Conserv. Biol.* **2010**, *9*, 54–60. [CrossRef]
28. Dutton, P.H.; Stewart, K. A method for sampling hatchling sea turtles for the development of a genetic tag. *MTN* **1995**, *138*, 3–7.
29. Faircloth, B.C. msatcommander: Detection of microsatellite repeat arrays and automated, locus-specific primer design. *Mol. Ecol. Resour.* **2008**, *8*, 92–94. [CrossRef]
30. Brownstein, M.J.; Carpten, J.D.; Smith, J.R. Modulation of non-templated nucleotide addition by Taq DNA polymerase: Primer modifications that facilitate genotyping. *Biotechniques* **1996**, *20*, 1004–1006. [CrossRef]
31. Edwards, T.; Goldberg, C.S.; Kaplan, M.E.; Schwalbe, C.R.; Swann, D.E. PCR primers for microsatellite loci in the desert tortoise (*Gopherus agassizii*, *Testudinidae*). *Mol. Ecol. Notes* **2003**, *3*, 589–591. [CrossRef]
32. King, T.L.; Julian, S.E. Conservation of microsatellite DNA flanking sequence across 13 emydid genera assayed with novel bog turtle (*Glyptemys muhlenbergii*) loci. *Conserv. Genet.* **2004**, *5*, 719–725. [CrossRef]
33. Schwartz, T.S.; Osentoski, M.; Lamb, T.; Karl, S.A. Microsatellite loci for the North American tortoises (genus Gopherus) and their applicability to other turtle species. *Mol. Ecol. Notes* **2003**, *3*, 283–286. [CrossRef]
34. Forlani, A.; Crestanello, B.; Mantovani, S.; Livoreil, B.; Zane, L.; Bertorelle, G.; Congiu, L. Identification and characterization of microsatellite markers in Hermann's tortoise (*Testudo hermanni*, *Testudinidae*). *Mol. Ecol. Notes* **2005**, *5*, 228–230. [CrossRef]
35. Perez, M.; Roger, B.; Lambourdiere, J.; Samadi, S.; Boisselier, M.C. Isolation and characterization of eight microsatellite loci for the study of gene flow between *Testudo marginata* and *Testudo weissingeri* (*Testudines*: *Testudinidae*). *Mol. Ecol. Notes* **2006**, *6*, 1096–1098. [CrossRef]
36. Kearse, M.; Moir, R.; Wilson, A.; Stones-Havas, S.; Cheung, M.; Sturrock, S.; Buxton, S.; Cooper, A.; Markowitz, S.; Duran, C.; et al. Geneious Basic: An integrated and extendable desktop software platform for the organization and analysis of sequence data. *Bioinformatics* **2012**, *28*, 1647–1649. [CrossRef] [PubMed]
37. Van Oosterhout, C.; Hutchinson, W.F.; Wills, D.P.M.; Shipley, P. micro-checker: Software for identifying and correcting genotyping errors in microsatellite data. *Mol. Ecol. Notes* **2004**, *4*, 535–538. [CrossRef]
38. Chapuis, M.P.; Estoup, A. Microsatellite null alleles and estimation of population differentiation. *Mol. Biol. Evol.* **2007**, *24*, 621–631. [CrossRef]
39. Rousset, F. genepop'007: A complete re-implementation of the genepop software for Windows and Linux. *Mol. Ecol. Resour.* **2008**, *8*, 103–106. [CrossRef]
40. Guo, S.W.; Thompson, E.A. Performing the Exact Test of Hardy-Weinberg Proportion for Multiple Alleles. *Biometrics* **1992**, *48*, 361–372. [CrossRef]
41. Rice, W.R. Analyzing tables of statistical tests. *Evolution* **1989**, *43*, 223–225. [CrossRef]
42. Yeh, F.C.; Yang, R.C.; Boyle, T.B.J.; Ye, Z.H.; Mao, J.X. *POPGENE, the User Friendly Shareware for Population Genetic Analysis*; Molecular Biology and Biotechnology Centre, University of Alberta: Edmonton, AB, Canada, 1997; Volume 10, pp. 295–301.
43. Pritchard, J.K.; Stephens, M.; Donnelly, P. Inference of population structure using multilocus genotype data. *Genetics* **2000**, *155*, 945–959. [CrossRef]
44. Francois, O.; Durand, E. Spatially explicit Bayesian clustering models in population genetics. *Mol. Ecol. Resour.* **2010**, *10*, 773–784. [CrossRef] [PubMed]
45. Evanno, G.; Regnaut, S.; Goudet, J. Detecting the number of clusters of individuals using the software STRUCTURE: A simulation study. *Mol. Ecol.* **2005**, *14*, 2611–2620. [CrossRef] [PubMed]
46. Earl, D.A.; vonHoldt, B.M. STRUCTURE HARVESTER: A website and program for visualizing STRUCTURE output and implementing the Evanno method. *Conserv. Genet. Resour.* **2012**, *4*, 359–361. [CrossRef]

47. Jakobsson, M.; Rosenberg, N.A. CLUMPP: A cluster matching and permutation program for dealing with label switching and multimodality in analysis of population structure. *Bioinformatics* **2007**, *23*, 1801–1806. [CrossRef]
48. Rosenberg, N. distruct: A program for the graphical display of population structure: PROGRAM NOTE. *Mol. Ecol. Notes* **2004**, *4*, 137–138. [CrossRef]
49. Weir, B.S.; Cockerham, C.C. Estimating F-Statistics for the Analysis of Population-Structure. *Evolution* **1984**, *38*, 1358–1370. [CrossRef]
50. Piry, S.; Alapetite, A.; Cornuet, J.-M.; Paetkau, D.; Baudouin, L.; Estoup, A. GENECLASS2: A Software for Genetic Assignment and First-Generation Migrant Detection. *J. Hered.* **2004**, *95*, 536–539. [CrossRef]
51. Rannala, B.; Mountain, J.L. Detecting immigration by using multilocus genotypes. *Proc. Natl. Acad. Sci. USA* **1997**, *94*, 9197–9201. [CrossRef] [PubMed]
52. Anadón, J.D.; Giménez, A.; Martínez, M.; Palazón, J.A.; Esteve, M.A. Assessing changes in habitat quality due to land use changes in the spur-thighed tortoise *Testudo graeca* using hierarchical predictive habitat models. *Divers. Distrib.* **2007**, *13*, 324–331. [CrossRef]
53. Anadón, J.; Giménez, A.; Graciá, E.; Pérez, I.; Ferrández, M.; Fahd, S.; El Mouden, H.; Kalboussi, M.; Jdeidi, T.; Larbes, S.; et al. Distribution of *Testudo graeca* in the western Mediterranean according to climatic factors. *Amphib.-Reptil.* **2012**, *33*, 285–296. [CrossRef]
54. Nekrasova, O.; Tytar, V.; Pupins, M.; Čeirāns, A.; Skute, A. GIS modelling of the distribution of terrestrial tortoise species: *Testudo graeca* and *Testudo hermanni* (*Testudines*, *Testudinidae*) of Eastern Europe in the context of climate change. *Zoodiversity* **2021**, *55*, 387–394. [CrossRef]
55. Zadhoush, B.; Rezaei, H.; Rajabizadeh, M. Distribution modeling and evaluation of the habitat integrity of *Testudo graeca zarudnyi* (*Testudines*: *Testudinidae*) in Central and Southeastern Iran. *J. Wildl. Biodivers.* **2021**, *5*, 15–27.
56. Hijmans, R.J.; Cameron, S.E.; Parra, J.L.; Jones, P.G.; Jarvis, A. Very high resolution interpolated climate surfaces for global land areas. *Int. J. Climatol.* **2005**, *25*, 1965–1978. [CrossRef]
57. Breiner, F.T.; Guisan, A.; Bergamini, A.; Nobis, M.P. Overcoming limitations of modelling rare species by using ensembles of small models. *Methods Ecol. Evol.* **2015**, *6*, 1210–1218. [CrossRef]
58. Breiner, F.T.; Nobis, M.P.; Bergamini, A.; Guisan, A. Optimizing ensembles of small models for predicting the distribution of species with few occurrences. *Methods Ecol. Evol.* **2018**, *9*, 802–808. [CrossRef]
59. Naimi, B. Package Usdm: Uncertainty Analysis for Species Distribution Models. 2017. Available online: https://cran.r-project.org/web/packages/usdm/usdm.pdf (accessed on 20 April 2024).
60. Broennimann, O.; Fitzpatrick, M.C.; Pearman, P.B.; Petitpierre, B.; Pellissier, L.; Yoccoz, N.G.; Thuiller, W.; Fortin, M.-J.; Randin, C.; Zimmermann, N.E.; et al. Measuring ecological niche overlap from occurrence and spatial environmental data. *Glob. Ecol. Biogeogr.* **2012**, *21*, 481–497. [CrossRef]
61. Nei, M. Estimation of average heterozygosity and genetic distance from a small number of individuals. *Genetics* **1978**, *89*, 583–590. [CrossRef] [PubMed]
62. Graciá, E.; Vargas-Ramírez, M.; Delfino, M.; Anadón, J.D.; Giménez, A.; Fahd, S.; Corti, C.; Jdeidi, T.B.; Fritz, U. Expansion after expansion: Dissecting the phylogeography of the widely distributed spur-thighed tortoise, *Testudo graeca* (*Testudines*: *Testudinidae*). *Biol. J. Linn. Soc.* **2017**, *121*, 641–654. [CrossRef]
63. Geffen, E.; Mendelssohn, H. Home range use and seasonal movements of the Egyptian tortoise (*Testudo kleinmanni*) in the northwestern Negev. *Herpetologica* **1988**, *44*, 354–359.
64. Díaz-Paniagua, C.; Keller, C.; Andreu, A.C. Annual variation of activity and daily distances moved in adult Spur-thighed tortoises, *Testudo graeca*, in southwestern Spain. *Herpetologica* **1995**, *51*, 225–233.
65. Cushman, S.; McKelvey, K.; Hayden, J.; Schwartz, M. Gene Flow in Complex Landscapes: Testing Multiple Hypotheses with Causal Modeling. *The Am. Nat.* **2006**, *168*, 486–499. [CrossRef]
66. Arakelyan, M.; Türkozan, O.; Hezaveh, N.; Parham, J. Ecomorphology of tortoises (*Testudo graeca* complex) from the Araks River Valley. *Russ. J. Herpetol.* **2018**, *25*, 245–252. [CrossRef]
67. Carretero, M.; Znari, M.; Harris, D.; Macé, J.C. Morphological divergence among populations of *Testudo graeca* from Westcentral Morocco. *Anim. Biol.* **2005**, *55*, 259–279. [CrossRef]
68. Lagarde, F.; Louzizi, T.; Slimani, T.; EL Mouden, H.; BEN Kaddour, K.; Moulherat, S.; Bonnet, X. Bushes protect tortoises from lethal overheating in arid areas of Morocco. *Environ. Conserv.* **2012**, *39*, 172–182. [CrossRef]

69. Bonnet, X.; Lagarde, F.; Henen, B.T.; Corbin, J.; Nagy, K.A.; Naulleau, G.; Balhoul, K.; Chastel, O.; Legrand, A.; Cambag, R. Sexual dimorphism in steppe tortoises (*Testudo horsfieldii*): Influence of the environment and sexual selection on body shape and mobility. *Biol. J. Linn. Soc.* **2001**, *72*, 357–372. [CrossRef]
70. Reydon, T.A.C. Are Species Good Units for Biodiversity Studies and Conservation Efforts? In *From Assessing to Conserving Biodiversity: History, Philosophy and Theory of the Life Sciences*; Casetta, E., Marques da Silva, J., Vecchi, D., Eds.; Springer: Cham, UK, 2019; Volume 24, pp. 167–193.